Enhancement of electron correlations in ion-gated FeSe film by *in situ* Seebeck and Hall measurements

Xu Zhang [1,2] Zhongpei Feng,[1,3] Xinjian Wei,[1,2] Zefeng Lin [1,2] Xingyu Jiang,[1,2] Wei Hu,[1] Zhongxu Wei,[1,2]
Mingyang Qin,[1,2] Juan Xu [1,4] Rui Xiong,[4] Jing Shi,[4] Jie Yuan,[1,5] Beiyi Zhu,[1] Qihong Chen [1,2] and Kui Jin [1,3,*]

[1]*Beijing National Laboratory for Condensed Matter Physics, Institute of Physics, Chinese Academy of Sciences, Beijing 100190, China*
[2]*School of Physical Sciences, University of Chinese Academy of Sciences, Beijing 100049, China*
[3]*Songshan Lake Materials Laboratory, Dongguan, Guangdong 523808, China*
[4]*School of Physics and Technology, Wuhan University, Wuhan 430072, China*
[5]*Key Laboratory of Vacuum Physics, School of Physical Sciences, University of Chinese Academy of Sciences, Beijing 100049, China*

In situ Seebeck and Hall measurements on FeSe films are carried out to understand the intrinsic evolution of the band structure as superconducting critical temperature (T_c) is tuned by ionic liquid gating. At the initial state, the nonmonotonous behavior of Hall and Seebeck curves indicates the multiband feature of FeSe film. As T_c increases via gating, the hole band gradually sinks below the Fermi level. Meanwhile, the Fermi energy of the electron band reduces while its carrier density increases, indicating that the electron band is flattening as T_c enhances. When T_c reaches the maximum at the final state, only the electron band exists and the effective electron mass is about $3.4m_e$.

I. INTRODUCTION

Ionic liquid gating (ILG) is a powerful technique to induce and tune superconductivity in transition metal dichalcogenides [1–4], cuprates [5–8], and iron-based superconductors [9–12]. Among these cases, FeSe has attracted intensive attention because its superconducting critical temperature (T_c) can be widely tuned from 8 K to more than 40 K [9–11], for which the ILG technique provides an opportunity to understand the nature of T_c enhancement. Previous studies on FeSe have shown that there is a close correlation between T_c and the band features [13–16]. However, since the ionic liquid on the sample surface is a barrier for surface-sensitive characterization techniques such as angle resolved photoemission spectroscopy (ARPES), the evolution of Fermi surface structure in ion-gated FeSe film hasn't been well studied yet.

In transport measurement, the Hall coefficient (R_H) is commonly used to extract the carrier density, which is linked to the Fermi wave vector in the Drude-Sommerfeld model with isotropic Fermi surface. Previously, the Hall measurements had been integrated with ILG technique to reveal the evolution of carrier density [8,11,12,17]. Seebeck measurement, as a complementary method, can assist in understanding the band structure in detail since it is directly related to Fermi energy. The Seebeck coefficient (S), also known as thermoelectric power, is a measure of entropy per quasiparticle. In Boltzmann theory, the Seebeck coefficient satisfies the function $S = \frac{\pi^2 k_B^2 T}{3q} \frac{1}{\varepsilon_F}$. Here, q is the charge of quasiparticle ($-e$ for electron and e for hole), k_B is the Boltzmann constant, and ε_F is the Fermi energy. In cuprates, the reconstructions of Fermi surface driven by the antiferromagnetic order [18] or charge density wave [19,20] have been revealed by Seebeck measurement. However, due to the technical complexity, combining Seebeck measurement with the ILG technique is experimentally challenging [21].

Here, we integrate both Seebeck and Hall measurements with ILG technique to study the evolution of Fermi surface structure in FeSe films. Before gating, the initial S/T, as well as R_H, first reduces and then enhances upon lowering the temperature, indicating a strong competition between electron and hole carriers. As T_c increases with ILG, both S/T and R_H curves move down and the upturns at low temperatures are gradually flattened. When T_c saturates at the final state, both S/T and R_H are independent of temperature indicating that the Fermi surface of the film possesses only the electron pocket at this temperature range. Then a clear physical picture can be drawn that the hole band gradually disappears as T_c increases. During this process, the monotonic decrease of S/T implies that the Fermi energy of the electron band is reducing, while the carrier density of the electron band at the final state is greatly enhanced compared to the initial state. Therefore, it can be reasonably deduced that the electron band is gradually flattened as T_c increases, which is also supported by its large effective electron mass at the final state.

II. EXPERIMENTS AND RESULTS

FeSe films with $\sim$200 nm in thickness were fabricated on LiF (001) substrates by pulsed laser deposition method [22]. Three samples with similar T_c's and transport properties were used in our experiments. Sample S1 was patterned into standard Hall bar and mounted between a heater and a cold

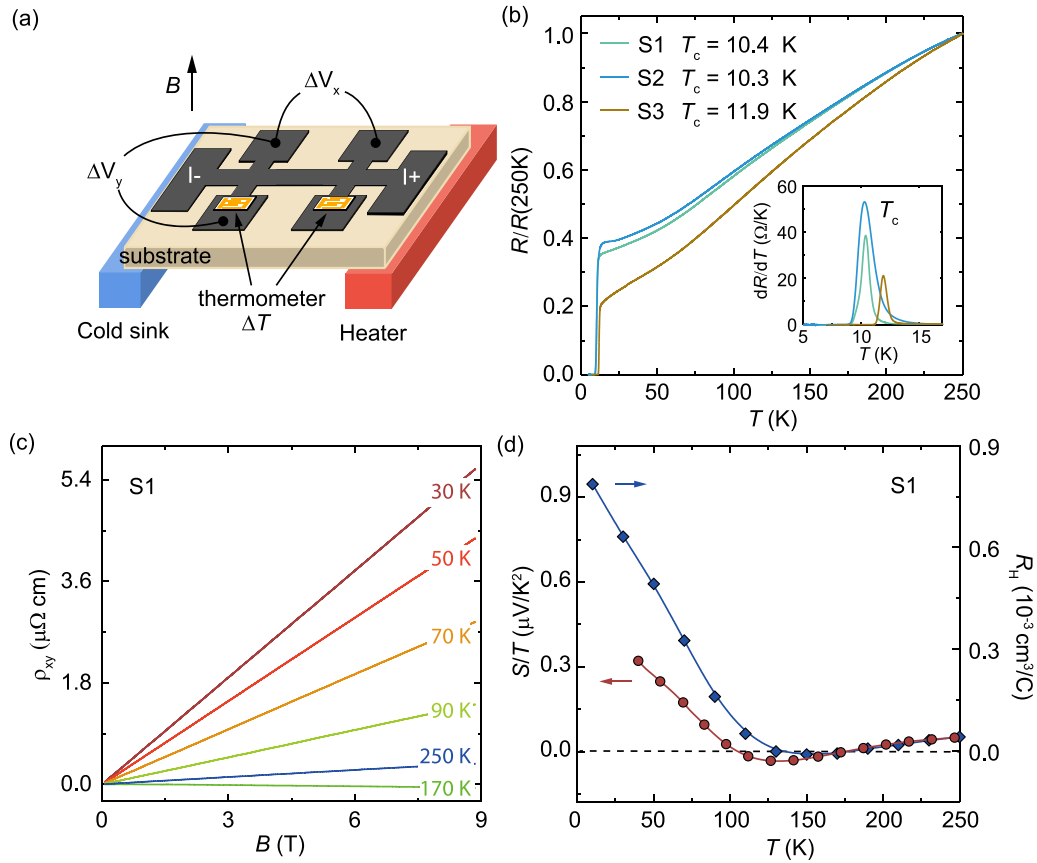*Corresponding author: kuijin@iphy.ac.cn

FIG. 1. (a) The schematic diagram of the device for Hall and Seebeck measurements. (b) The temperature dependence of resistance for three samples (S1–S3). Inset: the first derivative of resistance curves. (c) The field dependent Hall resistivity at different temperatures. (d) Temperature dependence of S/T and R_H for sample S1. The dashed line is a guide to the eye.

sink to carry out Hall and Seebeck measurements, as shown in Fig. 1(a). Electrical transport was measured with a physical property measurement system and a magnetic field was applied along the c axis of the sample during the measurement of Hall resistance. Thermoelectric measurements were performed in a Montana Cryostation system. A thin-film heater with 1 kΩ was attached to one end of the film to generate heat current. The other end was glued onto the copper cold platform with Ge varnish. The temperature difference $\Delta T (\sim 1$ K) was measured by a pair of thermometers. Sample S2 was used to measure the *in situ* Seebeck coefficient. The device for Seebeck measurements under ILG is shown in Fig. 2(a). The FeSe film covers half of the substrate, and the other half of the substrate is plated with gold as the gating electrode. Ionic liquid was dropped onto the substrate to bridge the sample and the gold electrode. The details of Hall measurements under ILG on sample S3 can be found in our previous work [8].

Figure 1(b) shows the temperature dependent normalized resistance [$R/R(250$ K)] of three FeSe samples (S1–S3). T_c's of these three samples are very close to each other, which are 10.4, 10.3, and 11.9 K, respectively. Here, T_c is defined as the temperature at which the first derivative of the $R(T)$ curve reaches the maximum as shown in the inset of Fig. 1(b). Figures 1(c) and 1(d) show the results of transport measurements for sample S1. The Hall resistivity of S1 is proportional to magnetic field at different temperatures, so the Hall co-

efficient can be calculated by the formula $R_H = \rho_{xy}/B$. As shown in Fig. 1(d), the dependence of R_H on temperature is consistent with previous results on FeSe film [10,11,23]. The Seebeck measurements are subsequently carried out on the same sample, and S/T displays similar behavior with R_H curve. At low temperatures, the positive signs of R_H and S/T indicate that hole carriers dominate the transport properties. As temperature increases, their values change significantly and undergo sign reversals twice, which implies a complicated competition between the hole and electron carriers in FeSe film.

Figure 2(b) shows the temperature dependent resistance of sample S2 under positive gate bias. With ionic gating, both the residual resistance ratio and T_c gradually increase. In general, ILG can induce both electrostatic [1–4] and electrochemical effects [6,8,24,25]. The former is limited by the Thomas-Fermi screening length, and thus only affects a layer of a few nanometers close to the sample surface. For the 200-nm-thick FeSe film in this study, the significant change of normal-state transport properties is beyond the capability of electrostatic effect. Particularly, the resistance at 200 K increases by $\sim$25%, which cannot be reached even if the surface layers (a few nanometers) are completely tuned to the insulating state. Therefore, the gating must be a bulk modulation dominated by electrochemical effect. It has been reported that water residuals are practically unavoidable in ionic liquid, and
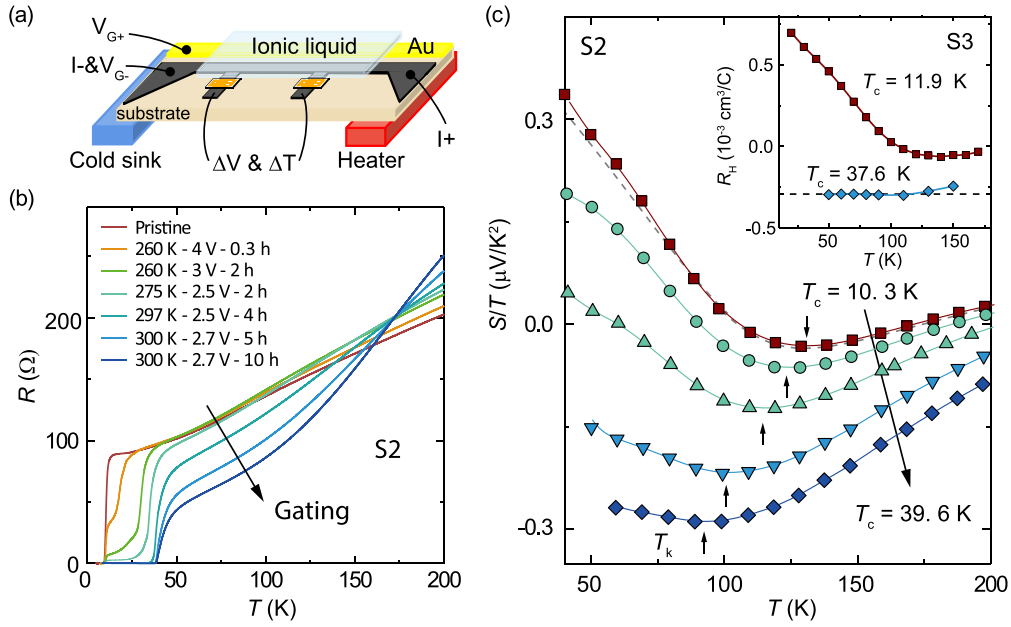
FIG. 2. (a) The schematic device structure for *in situ* Seebeck measurement combined with ILG technique. (b) The temperature dependent resistance with ILG for sample S2. (c) The temperature dependent S/T with ILG. The arrows point to the minima of S/T curves. The dashed line represents S/T of sample S1. Inset: The temperature dependent Hall coefficient in ILG for sample S3. The dashed line is a guide to the eye.

these water molecules dissociate into hydrogen and oxygen ions [25]. Under a positive gate bias, H^+ ions diffuse into the FeSe film and achieve the bulk modulation of the electronic properties of FeSe [26]. This process has been evidenced by NMR and magnetization measurements in series of Fe-based (i.e., 11 and 122 structures) superconductors. We note that electrochemical etching due to the reaction between the ionic liquid and the sample can be ignored, since the $R(T)$ curves do not rise up significantly during gating.

The temperature dependent S/T curves of sample S2 are obtained at each gating stage [Fig. 2(c)]. The feature of the initial S/T curve, which is similar to that of sample S1, has been described above. Here, as T_c increases, two features of the evolution of the S/T curve can be clearly recognized. One is that the whole curve moves down and the values of S/T within the entire temperature range become negative eventually. The other is that the upturn at low temperatures is suppressed especially in the final state. The temperature dependent Hall coefficients of sample S3 at the initial and final states are shown in the inset of Fig. 2(c). Obviously, the evolution of the $R_H(T)$ curve with T_c is similar to that of S/T curves.

III. DISCUSSION

The Fermi surface of bulk FeSe consists of hole pockets around the Γ point and electron pockets around the M point [27,28]. To elaborate on the information of band structure from Seebeck and Hall measurements, the Boltzmann equation in the presence of both electron- and hole-type carriers is considered [29]. In this two-band model, the Hall coefficient is written as

$$R_H = \frac{1}{e} \frac{\left(\mu_h^2 n_h - \mu_e^2 n_e\right) - (\mu_e \mu_h)^2 B^2 (n_h - n_e)}{\left(\mu_h n_h + \mu_e n_e\right)^2 + (\mu_e \mu_h)^2 B^2 (n_h - n_e)^2} \quad (1)$$

and the S/T is described by

$$\frac{S}{T} = \frac{\pi^2 k_B^2}{3e} \frac{\mu_h n_h / \varepsilon_F^h - \mu_e n_e / \varepsilon_F^e}{\mu_h n_h + \mu_e n_e}, \quad (2)$$

where ε_F^h (ε_F^e), μ_h (μ_e), and n_h (n_e) stand for the Fermi energy, the mobility, and the carrier density of hole (electron), respectively. Since the Hall resistivity is proportional to magnetic field in the whole temperature range [Fig. 1(c)], the square term of the magnetic field can be ignored and Eq. (1) is simplified as

$$R_H = \frac{1}{e} \frac{\left(\mu_h^2 n_h - \mu_e^2 n_e\right)}{\left(\mu_h n_h + \mu_e n_e\right)^2}. \quad (3)$$

The dependence of S/T and R_H on temperature are determined by the competition between electron and hole carriers. As a result, these two curves display similar behavior as shown in Fig. 1(d). At the high temperature region, the positive S/T and R_H indicate that the hole carriers dominate the transport properties. With decreasing temperature, the monotonous decrease of S/T and R_H suggest the contribution of electron carriers grows faster than hole carriers. However, the tendency of both curves changes at a specific temperature which is denoted as T_k (the location of the minimum). The S/T and R_H curves display an upturn behavior below this temperature, indicating that the contribution of hole carriers increases in transport.

The nonmonotonic behaviors in Hall and Seebeck measurements are inherent in the pristine FeSe compound. No matter whether for single crystal, thin film, or chemically doped FeSe, the minima of S/T and R_H appear in the range 100–150 K [11,21,30,31]. The extreme points in the temperature dependence of Seebeck and Hall coefficient curves have

been thoroughly studied in cuprates [18,19,32,33], which are attributed to the Fermi surface reconstruction resulting from the formation of charge density wave or antiferromagnetic order. In analogy, there seems to be a change of Fermi surface structure in the FeSe compound occurring at T_k, below which the scattering mechanism changes. T_k at the initial state is equal to 135 K, which locates at the temperature region where the nematic order in FeSe system emerges [28,34–36]. The nematic order, which is always intertwined with structure transition and band splitting, can induce significant changes in band structure and consequently lead to the complex behavior of S/T. For single crystals, a "kink" anomaly occurs in the $R(T)$ curves [37–39]. Although this kink behavior is not observed in FeSe films [10,11,23], the band splitting is still present [40]. Moreover, the in-plane angular magnetoresistance of FeSe film shows a twofold symmetry at low temperatures [41]. Thus, it is likely that the nematic order is present in the film and results in the change of Fermi surface structure at T_k.

During gating, the upturn behavior is gradually suppressed and the values of S/T change from positive to negative [Fig. 2(c)]. At the final state, both S/T and R_H curves are almost temperature independent. This behavior is a typical feature of single band, which can be understood from Eqs. (2) and (3) in the case that the hole carrier density reduces to zero. Then, the Fermi energy of this electron band can be estimated to be 84.4 meV by the formula $S/T = -\frac{\pi^2 k_B^2}{3e}\frac{1}{\varepsilon_F}$. Such a result is consistent with the ARPES results of K-dosed FeSe [15] in which only the electron pocket around the M point is detected. Hence, it is reasonable to conclude that the hole band sinks below the Fermi level gradually with gating. In order to quantitatively characterize this process, $\Delta S/T = S/T(60 \text{ K}) - S/T(T_k)$ is used to describe the weight of hole carriers in transport at low temperatures. As shown in Fig. 3(a), the $\Delta S/T$ decreases gradually with gating. When $\Delta S/T = 0$, the hole pocket disappears, suggestive of a Lifshitz transition.

In addition to the upturn behavior, the value of the Seebeck coefficient at T_k also shows a correlation with gating. The large negative $S(T_k)$ has been detected in FeSe thin film, which is attributed to a large effective electron mass (m^*) of electron carriers [21]. In our ILG experiments, growing $|S(T_k)|$ is unambiguously observed. For single band systems, S/T is inversely proportional to ε_F according to the Boltzmann equation, while for multiband systems it is more complicated since it can be affected by the relative weight of the electron and hole band. As aforementioned, with ionic gating the hole bands gradually disappear and the carrier density of electron increases by an order of magnitude, which means that the transport is dominated by the electron band. Particularly, for the bottom two S/T curves in Fig. 2(c), the upturn behaviors have almost been suppressed, i.e., the hole band has vanished, but the last curve shows significantly higher $|S/T|$ compared to the second-to-last one. The increase of $|S/T|$ suggests the Fermi energy of the electron band decreases with electron doping. To describe the structure of electron bands, Fig. 3(a) displays the evolution of the Fermi energy calculated from $S/T(T_k)$ during the gating process. With the enhancement of T_c, the Fermi energy gradually decreases and is about 84.4 meV when T_c saturates.
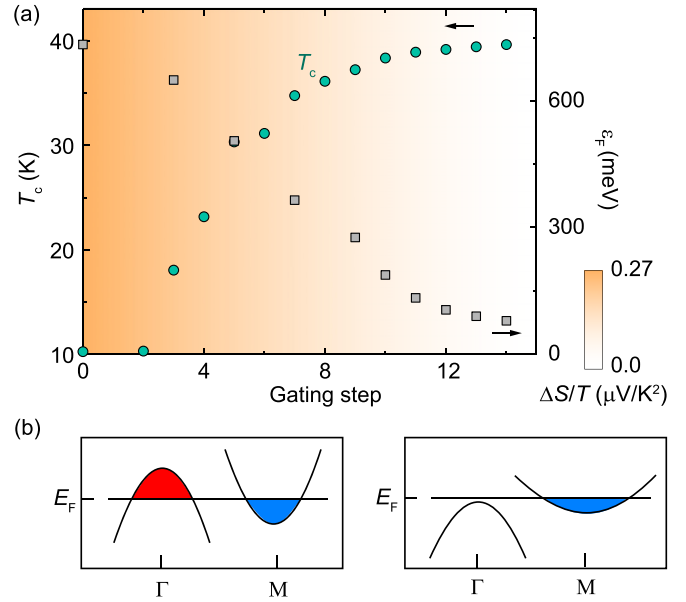

FIG. 3. (a) With gating process, T_c is gradually saturated as $\Delta S/T$ is suppressed to zero. The corresponding Fermi energy calculated from $S/T(T_k)$ is negatively correlated with T_c. At final state, the Fermi energy of electron band is equal to 84.4 meV. (b) The evolution of band structure with gating process.

As for the density of electrons, two-band fitting for the field dependence of both transverse and longitudinal resistivities [42] suggests that the electron density of pristine FeSe film (S3) is about 9.5×10^{19} cm^{-3} at 60 K, as shown in Table I. At final state this value reaches 2.1×10^{21} cm^{-3} calculated by the Hall coefficient, implying the significant increase of electron density during gating. Thus, the large increase of electron density yet with decreased Fermi energy of electron band points to a flat band scenario. Based on the Sommerfeld theory [43], the Fermi energy in 2D system satisfies as $\varepsilon_F = \frac{\hbar^2(2\pi n_s)}{2m^*}$ and the m^* of the electron at final state is calculated to be $3.4 m_e$. Here, n_s is the surface carrier density. The large effective electron mass also strongly supports the flat band picture. In addition, more transport parameters could be calculated by a combination of Hall and Seebeck coefficients, which are also shown in Table I.

Now, a relatively complete picture for the evolution of band structure has been established in ion-gated FeSe as summarized in Fig. 3(b). With increasing T_c, the changes of the band structure include two parts: one is that the hole band at the Γ point sinks below the Fermi level, corresponding to the Lifshitz transition; the other is that the electron correlation increases, manifesting as the flattening of the electron band at the M point. The Lifshitz transition accompanying a sudden jump of T_c from 8 to 30 K in the FeSe compound has been reported in previous ILG and ARPES experiments [11,14], therefore the change of Fermi surface topology is considered to be the reason for the dramatic increase of T_c. In our study, however, the continuous changes in T_c, $S/T(T_k)$, and R_H indicate that the electron correlation is also intimately correlated with the enhancement of T_c. As shown in Fig. 3(a), T_c first increases dramatically while the Fermi energy changes strongly, and it tends to saturate

TABLE I. Transport parameters of pristine and gated FeSe at 60 K.

T_c (K)	n_e (cm^{-3})	n_h (cm^{-3})	μ_e (m²/V s)	μ_h (m²/V s)	m^* (m_e)	k_F (m⁻¹)	v_F (m/s)	τ (s)	l (nm)
$\sim$11 K	9.5×10^{19}	1.1×10^{-20}	1.2×10^{-2}	1.2×10^{-2}					
$\sim$39 K	2.1×10^{21}		2.0×10^{-3}		3.4	2.7×10^{9}	9.2×10^{4}	3.9×10^{-14}	3.6

as the Fermi energy saturates. This synchronized behavior provides support for an electron-correlation-mediated superconducting mechanism. The flat band is also observed in other electron-doped FeSe films by ARPES measurements [13,15]. For Na-dosed FeSe, the effective mass increases to $2.7 m_e$, when T_c is 20 K. And for K-dosed FeSe, the effective mass is $4 m_e$ for the superconducting state with a T_c of 40 K. The surface-doped K$^+$ ions induce local electric field, which limits the hopping between Fe atoms and narrows the bandwidth [44]. The H$^+$ ions injected by ionic liquid may play a similar role to the K$^+$ ions and lead to the enhancement of electron correlations. Recently, spin fluctuations have been revealed by inelastic neutron scattering in FeSe [45–47]. A spin resonance develops in the superconducting state [47], giving strong evidence for a spin-fluctuation-mediated superconducting pairing mechanism. In this scenario, the superconducting pairing amplitude is determined by the strength of electron correlations [48,49]. Nevertheless, it should be noted that for a multiband system like FeSe, ionic gating inevitably affects both the carrier concentration and the band structure. Therefore, it is difficult to disentangle the relative importance of increasing electron density and reduced bandwidth on T_c from transport measurements. Further studies are required to conclusively determine the specific role of increasing electron density on superconductivity in FeSe besides electron correlation.

In summary, we have combined an ILG technique with electrical and thermal transport measurements to study FeSe thin films. The evolution of Fermi surface structure has been revealed in FeSe thin film under the ILG. As the T_c of the film is continuously enhanced from 10 to 40 K, the hole band gradually sinks below the Fermi surface and the electron band flattens. The *in situ* measurements break the limit of ILG and provide a controllable method to study the material properties, which is worthy of being extended to other research.

[1] J. T. Ye, Y. J. Zhang, R. Akashi, M. S. Bahramy, R. Arita, and Y. Iwasa, Superconducting dome in a gate-tuned band insulator, Science **338**, 1193 (2012).

[2] W. Shi, J. Ye, Y. Zhang, R. Suzuki, M. Yoshida, J. Miyazaki, N. Inoue, Y. Saito, and Y. Iwasa, Superconductivity series in transition metal dichalcogenides by ionic gating, Sci. Rep. **5**, 12534 (2015).

[3] Q. H. Chen, J. M. Lu, L. Liang, O. Zheliuk, A. Ali, P. Sheng, and J. T. Ye, Inducing and Manipulating Heteroelectronic States in a Single MoS$_2$ Thin Flake, Phys. Rev. Lett. **119**, 147002 (2017).

[4] Q. Chen, J. Lu, L. Liang, O. Zheliuk, A. Ali El Yumin, and J. Ye, Continuous low-bias switching of superconductivity in a MoS$_2$ transistor, Adv. Mater. **30**, e1800399 (2018).

[5] A. T. Bollinger, G. Dubuis, J. Yoon, D. Pavuna, J. Misewich, and I. Bozovic, Superconductor-insulator transition in La$_{2-x}$Sr$_x$CuO$_4$ at the pair quantum resistance, Nature (London) **472**, 458 (2011).

[6] M. Rafique, Z. Feng, Z. Lin, X. Wei, M. Liao, D. Zhang, K. Jin, and Q. K. Xue, Ionic liquid gating induced protonation of electron-doped cuprate superconductors, Nano Lett. **19**, 7775 (2019).

[7] X. Leng, J. Garcia-Barriocanal, S. Bose, Y. Lee, and A. M. Goldman, Electrostatic Control of the Evolution from a Superconducting Phase to an Insulating Phase in Ultrathin YBa$_2$Cu$_3$O$_{7-x}$ Films, Phys. Rev. Lett. **107**, 027001 (2011).

[8] X. Wei, H.-B. Li, Q. Zhang, D. Li, M. Qin, L. Xu, W. Hu, Q. Huan, L. Yu, J. Miao, J. Yuan, B. Zhu, A. Kusmartseva, F. V. Kusmartsev, A. V. Silhanek, T. Xiang, W. Yu, Y. Lin, L. Gu, P. Yu, Q. Chen, and K. Jin, A selective control of volatile and non-volatile superconductivity in an insulating copper oxide via ionic liquid gating, Sci. Bull. **65**, 1607 (2020).

[9] N. Shikama, Y. Sakishita, F. Nabeshima, Y. Katayama, K. Ueno, and A. Maeda, Enhancement of superconducting transition temperature in electrochemically etched FeSe/LaAlO$_3$ films, Appl. Phys. Express **13**, 083006 (2020).

[10] J. Shiogai, Y. Ito, T. Mitsuhashi, T. Nojima, and A. Tsukazaki, Electric-field-induced superconductivity in electrochemically etched ultrathin FeSe films on SrTiO$_3$ and MgO, Nat. Phys. **12**, 42 (2015).

[11] B. Lei, J. H. Cui, Z. J. Xiang, C. Shang, N. Z. Wang, G. J. Ye, X. G. Luo, T. Wu, Z. Sun, and X. H. Chen, Evolution of High-Temperature Superconductivity from a Low-T_c Phase Tuned by Carrier Concentration in FeSe Thin Flakes, Phys. Rev. Lett. **116**, 077002 (2016).

[12] K. Hanzawa, H. Sato, H. Hiramatsu, T. Kamiya, and H. Hosono, Electric field-induced superconducting transition of insulating

FeSe thin film at 35 K, Proc. Natl. Acad. Sci. USA **113**, 3986 (2016).

[13] J. J. Seo, B. Y. Kim, B. S. Kim, J. K. Jeong, J. M. Ok, J. S. Kim, J. D. Denlinger, S. K. Mo, C. Kim, and Y. K. Kim, Superconductivity below 20 K in heavily electron-doped surface layer of FeSe bulk crystal, Nat. Commun. **7**, 11116 (2016).

[14] X. Shi, Z. Q. Han, X. L. Peng, P. Richard, T. Qian, X. X. Wu, M. W. Qiu, S. C. Wang, J. P. Hu, Y. J. Sun, and H. Ding, Enhanced superconductivity accompanying a Lifshitz transition in electron-doped FeSe monolayer, Nat. Commun. **8**, 14988 (2017).

[15] C. H. Wen, H. C. Xu, C. Chen, Z. C. Huang, X. Lou, Y. J. Pu, Q. Song, B. P. Xie, M. Abdel-Hafiez, D. A. Chareev, A. N. Vasiliev, R. Peng, and D. L. Feng, Anomalous correlation effects and unique phase diagram of electron-doped FeSe revealed by photoemission spectroscopy, Nat. Commun. **7**, 10840 (2016).

[16] Y. Miyata, K. Nakayama, K. Sugawara, T. Sato, and T. Takahashi, High-temperature superconductivity in potassium-coated multilayer FeSe thin films, Nat. Mater. **14**, 775 (2015).

[17] J. Shiogai, T. Miyakawa, Y. Ito, T. Nojima, and A. Tsukazaki, Unified trend of superconducting transition temperature versus Hall coefficient for ultrathin FeSe films prepared on different oxide substrates, Phys. Rev. B **95**, 115101 (2017).

[18] P. R. Mandal, T. Sarkar, and R. L. Greene, Anomalous quantum criticality in the electron-doped cuprates, Proc. Natl. Acad. Sci. USA **116**, 5991 (2019).

[19] S. Badoux, S. A. A. Afshar, B. Michon, A. Ouellet, S. Fortier, D. LeBoeuf, T. P. Croft, C. Lester, S. M. Hayden, H. Takagi, K. Yamada, D. Graf, N. Doiron-Leyraud, and L. Taillefer, Critical Doping for the Onset of Fermi-Surface Reconstruction by Charge-Density-Wave Order in the Cuprate Superconductor $La_{2-x}Sr_xCuO_4$, Phys. Rev. X **6**, 021004 (2016).

[20] O. Cyr-Choinière, S. Badoux, G. Grissonnanche, B. Michon, S. A. A. Afshar, S. Fortier, D. LeBoeuf, D. Graf, J. Day, D. A. Bonn, W. N. Hardy, R. Liang, N. Doiron-Leyraud, and L. Taillefer, Anisotropy of the Seebeck Coefficient in the Cuprate Superconductor $YBa_2Cu_3O_y$: Fermi-Surface Reconstruction by Bidirectional Charge Order, Phys. Rev. X **7**, 031042 (2017).

[21] S. Shimizu, J. Shiogai, N. Takemori, S. Sakai, H. Ikeda, R. Arita, T. Nojima, A. Tsukazaki, and Y. Iwasa, Giant thermoelectric power factor in ultrathin FeSe superconductor, Nat. Commun. **10**, 825 (2019).

[22] Z. Feng, J. Yuan, G. He, W. Hu, Z. Lin, D. Li, X. Jiang, Y. Huang, S. Ni, J. Li, B. Zhu, X. Dong, F. Zhou, H. Wang, Z. Zhao, and K. Jin, Tunable critical temperature for superconductivity in FeSe thin films by pulsed laser deposition, Sci. Rep. **8**, 4039 (2018).

[23] Y. Imai, Y. Sawada, F. Nabeshima, D. Asami, M. Kawai, and A. Maeda, Control of structural transition in $FeSe_{1-x}Te_x$ thin films by changing substrate materials, Sci. Rep. **7**, 46653 (2017).

[24] A. M. Perez-Munoz, P. Schio, R. Poloni, A. Fernandez-Martinez, A. Rivera-Calzada, J. C. Cezar, E. Salas-Colera, G. R. Castro, J. Kinney, C. Leon, J. Santamaria, J. Garcia-Barriocanal, and A. M. Goldman, In operando evidence of deoxygenation in ionic liquid gating of $YBa_2Cu_3O_{7-X}$, Proc. Natl. Acad. Sci. USA **114**, 215 (2017).

[25] N. Lu, P. Zhang, Q. Zhang, R. Qiao, Q. He, H. B. Li, Y. Wang, J. Guo, D. Zhang, Z. Duan, Z. Li, M. Wang, S. Yang, M. Yan, E. Arenholz, S. Zhou, W. Yang, L. Gu, C. W. Nan, J. Wu, Y. Tokura, and P. Yu, Electric-field control of tri-state phase transformation with a selective dual-ion switch, Nature (London) **546**, 124 (2017).

[26] Y. Cui, G. Zhang, H. Li, H. Lin, X. Zhu, H.-H. Wen, G. Wang, J. Sun, M. Ma, Y. Li, D. Gong, T. Xie, Y. Gu, S. Li, H. Luo, P. Yu, and W. Yu, Protonation induced high-T_c phases in iron-based superconductors evidenced by NMR and magnetization measurements, Sci. Bull. **63**, 11 (2018).

[27] A. I. Coldea and M. D. Watson, The key ingredients of the electronic structure of FeSe, Annu. Rev. Condens. Matter Phys. **9**, 125 (2018).

[28] M. D. Watson, T. K. Kim, A. A. Haghighirad, N. R. Davies, A. McCollam, A. Narayanan, S. F. Blake, Y. L. Chen, S. Ghannadzadeh, A. J. Schofield, M. Hoesch, C. Meingast, T. Wolf, and A. I. Coldea, Emergence of the nematic electronic state in FeSe, Phys. Rev. B **91**, 155106 (2015).

[29] K. Behnia, D. Jaccard, and J. Flouquet, On the thermoelectricity of correlated electrons in the zero-temperature limit, J. Phys.: Condens. Matter **16**, 5187 (2004).

[30] E. L. Thomas, W. Wong-Ng, D. Phelan, and J. N. Millican, Thermopower of Co-doped FeSe, J. Appl. Phys. **105**, 073906 (2009).

[31] M. D. Watson, T. Yamashita, S. Kasahara, W. Knafo, M. Nardone, J. Beard, F. Hardy, A. McCollam, A. Narayanan, S. F. Blake, T. Wolf, A. A. Haghighirad, C. Meingast, A. J. Schofield, H. Lohneysen, Y. Matsuda, A. I. Coldea, and T. Shibauchi, Dichotomy Between the Hole and Electron Behavior in Multiband Superconductor FeSe Probed by Ultrahigh Magnetic Fields, Phys. Rev. Lett. **115**, 027006 (2015).

[32] T. Sarkar, P. R. Mandal, J. S. Higgins, Y. Zhao, H. Yu, K. Jin, and R. L. Greene, Fermi surface reconstruction and anomalous low-temperature resistivity in electron-doped $La_{2-x}Ce_xCuO_4$, Phys. Rev. B **96**, 155449 (2017).

[33] N. Doiron-Leyraud, S. Lepault, O. Cyr-Choinière, B. Vignolle, G. Grissonnanche, F. Laliberté, J. Chang, N. Barišić, M. K. Chan, L. Ji, X. Zhao, Y. Li, M. Greven, C. Proust, and L. Taillefer, Hall, Seebeck, and Nernst Coefficients of Underdoped $HgBa_2CuO_{4+\delta}$: Fermi-Surface Reconstruction in an Archetypal Cuprate Superconductor, Phys. Rev. X **3**, 021019 (2013).

[34] Y. Zhang, M. Yi, Z. K. Liu, W. Li, J. J. Lee, R. G. Moore, M. Hashimoto, M. Nakajima, H. Eisaki, S. K. Mo, Z. Hussain, T. P. Devereaux, Z. X. Shen, and D. H. Lu, Distinctive orbital anisotropy observed in the nematic state of a FeSe thin film, Phys. Rev. B **94**, 115153 (2016).

[35] T. Shimojima, Y. Suzuki, T. Sonobe, A. Nakamura, M. Sakano, J. Omachi, K. Yoshioka, M. Kuwata-Gonokami, K. Ono, H. Kumigashira, A. E. Böhmer, F. Hardy, T. Wolf, C. Meingast, H. v. Löhneysen, H. Ikeda, and K. Ishizaka, Lifting of xz/yz orbital degeneracy at the structural transition in detwinned FeSe, Phys. Rev. B **90**, 121111(R) (2014).

[36] K. Nakayama, Y. Miyata, G. N. Phan, T. Sato, Y. Tanabe, T. Urata, K. Tanigaki, and T. Takahashi, Reconstruction of Band Structure Induced by Electronic Nematicity in an FeSe Superconductor, Phys. Rev. Lett. **113**, 237001 (2014).

[37] M. L. Amigó, V. A. Crivillero, D. G. Franco, and G. Nieva, Multiband character of β-FeSe: Angular dependence of the magnetoresistance and upper critical field, J. Phys.: Conf. Ser. **568**, 022005 (2014).

[38] K. K. Huynh, Y. Tanabe, T. Urata, H. Oguro, S. Heguri, K. Watanabe, and K. Tanigaki, Electric transport of a single-crystal iron chalcogenide FeSe superconductor: Evidence of symmetry-breakdown nematicity and additional ultrafast Dirac cone-like carriers, Phys. Rev. B **90**, 144516 (2014).

[39] S. Knöner, D. Zielke, S. Köhler, B. Wolf, T. Wolf, L. Wang, A. Böhmer, C. Meingast, and M. Lang, Resistivity and magnetoresistance of FeSe single crystals under helium-gas pressure, Phys. Rev. B **91**, 174510 (2015).

[40] B. Shen, Z. Feng, J.-W. Huang, Y. Hu, Q. Gao, C. Li, Y. Xu, G.-D. Liu, L. Yu, L. Zhao, K. Jin, and X. J. Zhou, Electronic structure and nematic phase transition in superconducting multiple-layer FeSe films grown by pulsed laser deposition method, Chin. Phys. B **26**, 077402 (2017).

[41] Z. Feng, High-throughput investigations of superconducting combinatorial films, Doctor of Philosophy in condensed matter physics, University of Chinese Academy of Sciences, 2019.

[42] Z. Feng, J. Yuan, J. Li, X. Wu, W. Hu, B. Shen, M. Qin, L. Zhao, B. Zhu, V. Stanev, M. Liu, G. Zhang, X. Dong, F. Zhou, X. Zhou, J. Hu, I. Takeuchi, Z. Zhao, and K. Jin, High-throughput investigation of tunable superconductivity in FeSe films, arXiv:1807.01273.

[43] N. W. Ashcroft and N. D. Mermin, *Solid State Physics* (Saunders, Philadelphia, 1976), pp. 36–37.

[44] Y. W. Choi and H. J. Choi, Role of Electric Fields on Enhanced Electron Correlation in Surface-Doped FeSe, Phys. Rev. Lett. **122**, 046401 (2019).

[45] M. C. Rahn, R. A. Ewings, S. J. Sedlmaier, S. J. Clarke, and A. T. Boothroyd, Strong $(\pi, 0)$ spin fluctuations in β–FeSe observed by neutron spectroscopy, Phys. Rev. B **91**, 180501(R) (2015).

[46] Q. Wang, Y. Shen, B. Pan, X. Zhang, K. Ikeuchi, K. Iida, A. D. Christianson, H. C. Walker, D. T. Adroja, M. Abdel-Hafiez, X. Chen, D. A. Chareev, A. N. Vasiliev, and J. Zhao, Magnetic ground state of FeSe, Nat. Commun. **7**, 12182 (2016).

[47] Q. Wang, Y. Shen, B. Pan, Y. Hao, M. Ma, F. Zhou, P. Steffens, K. Schmalzl, T. R. Forrest, M. Abdel-Hafiez, X. Chen, D. A. Chareev, A. N. Vasiliev, P. Bourges, Y. Sidis, H. Cao, and J. Zhao, Strong interplay between stripe spin fluctuations, nematicity and superconductivity in FeSe, Nat. Mater. **15**, 159 (2016).

[48] R. Yu, P. Goswami, Q. Si, P. Nikolic, and J. X. Zhu, Superconductivity at the border of electron localization and itinerancy, Nat. Commun. **4**, 2783 (2013).

[49] C. Fang, Y.-L. Wu, R. Thomale, B. A. Bernevig, and J. Hu, Robustness of s-Wave Pairing in Electron-Overdoped $A_{1-y}Fe_{2-x}Se_2$ (A=K, Cs), Phys. Rev. X **1**, 011009 (2011).